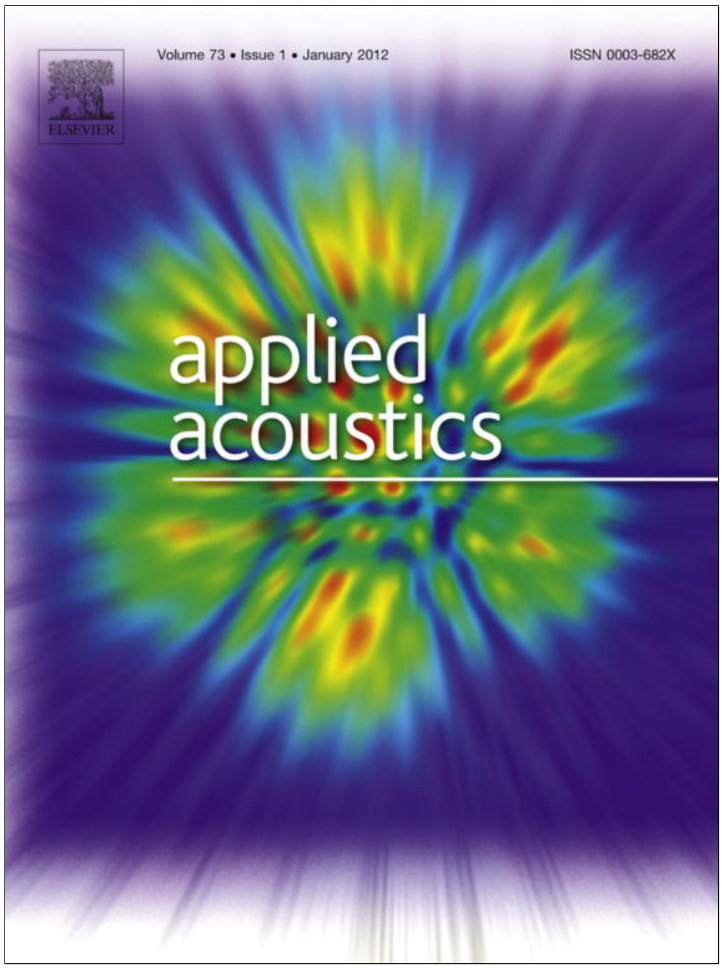

Applied Acoustics 73 (2012) 72–77

Contents lists available at ScienceDirect

Applied Acoustics

journal homepage: www.elsevier.com/locate/apacoust

Technical Note

Insulation room for aero-acoustic experiments at moderate Reynolds and low Mach numbers

A. Van Hirtum *, Y. Fujiso

GIPSA-lab, UMR CNRS 5216, Grenoble University, France

ARTICLE INFO

Article history:
Received 12 November 2010
Received in revised form 24 June 2011
Accepted 27 June 2011
Available online 27 July 2011

Keywords:
Anechoic room
Aero-acoustics

ABSTRACT

A non-expensive insulation box for aero-acoustic experiments at moderate Reynolds numbers $Re < 2 \times 10^4$ and low Mach numbers $M < 0.2$ is presented. Its performance is evaluated with particular attention to unwanted noise sources inherent to the flow facility. Objective acoustic parameters of the insulation box are assessed.

1. Introduction

The current technical note results from the need to perform aero-acoustic experiments in an ordinary laboratory room equipped with a flow facility. The flow facility consists of compressed air circulating in a uniform tube with diameter 1 cm for which the volume flow rate can be imposed by means of a pressure regulator (Norgren type 11-818-987) and a manual valve. The oil-injected rotary screw compressor (Copco GA7) is isolated in a separated room. The geometries and volume flow rates of interest are such that studied flows are characterised by moderate Reynolds numbers $Re < 2 \times 10^4$ and low Mach numbers $M < 0.2$. Sound frequencies of interest are less than 10 kHz.

The presence of the pressure regulator and airflow circuit in the room is a source of constant broadband background noise, which cannot be filtered out using basic signal processing techniques since it affects all frequencies. Additional constant noise sources are due to the experimental procedure such as computers ventilation noise during data acquisition. Besides unwanted noise sources inherent to the airflow facility or experimental procedure, several punctual and random unwanted noise sources are related to inside activities of colleagues or outdoor activities of passengers or traffic. Consequently, instead of isolating individual noise sources it has been chosen to integrate a non-expensive experimental box in the ordinary room which is suitable for aero-acoustic experiments for flows in the range of interest and serves as an insulation room.

In the following, the design of the insulation box is outlined and its performance is evaluated in terms of insulation and quantitative objective acoustic parameters. The design of the box is successful in case noise produced during aero-acoustic experiments at moderate Reynolds and low Mach numbers can be studied in acceptable flow and acoustic conditions.

2. Design and instrumentation

The box is inserted in an ordinary room with no acoustical treatment of volume 49.8 m^3 and dimensions $4.45 \times 4 \times 2.80$ m, length $\times$ width $\times$ height. Due to the location of windows, entrance door, space required for experimental material and instruments (such as the settling chamber for flow experiments) and manufacturing issues, the external dimensions of the box are reduced to $2.07 \times 2.10 \times 2.14$ m, length $\times$ width $\times$ height. A two-dimensional spatial overview of the ordinary room and insulation box is given in Fig. 1a.

The insulation box is built in rigid flat wooden fibre board insulation panels with thickness 2.5 cm to which acoustic foam (SE50-AL-ML, Elastomeres Solutions) with thickness 5 cm is added. The foam consists out of a basis layer of PVC (polyvinyl chloride 5 kg/m^2) to which PU ether (polyurethane) is added. Therefore, the final insulation panels of the insulation box are three layered – wood, PVC, PU ether – with a total thickness of 7.5 cm as illustrated in Fig. 1b. The foam absorbs frequencies in the range from 100 up to 10 kHz which is 'a priori' suitable for broadband noise sources such as pressure regulator and PC ventilator. The efficiency of the acoustic foam depends on the noise frequencies. Characteristics of the insulation box are summarised in Table 1.

Three trapdoors allow access for instrumentation cables. In addition, trapdoors can be used to insert the nozzle to be studied. Trapdoors are made of the same rigid wood panels as the box and

* Corresponding author.
E-mail address: annemie.vanhirtum@gipsa-lab.grenoble-inp.fr (A. Van Hirtum).

0003-682X/$ - see front matter © 2011 Elsevier Ltd. All rights reserved.
doi:10.1016/j.apacoust.2011.06.014

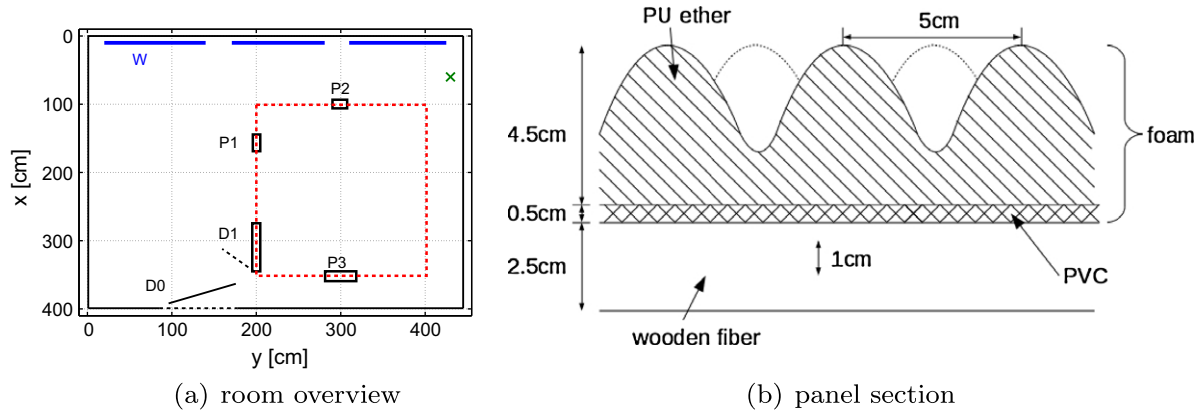

(a) room overview (b) panel section

Fig. 1. (a) Two-dimensional spatial overview of experimental room without acoustical treatment with entrance *D*0, room windows *W*, compressed air supply ×, insulation box (dashed rectangle) equipped with 3 trapdoors *P* and door access *D*1. (b) Illustration of a section of the three-layered insulation panel.

Table 1
Relevant insulation box characteristics. Internal dimensions correspond to length, $L_x \times$ width, $L_y \times$ height, L_z. Corresponding values of the absorption coefficient of the foam α_f for different frequency ranges are indicated [1].

	Values and range	
Internal dimensions	$L_x = 1.92$ m, $L_y = 1.95$ m, $L_z = 1.99$ m	
Internal volume, V	7.45 m^3	
Internal wall surface, S	22.9 m^2	
Absorbing foam (Elastomeres Solutions) (SE50-AL-ML)	98% ($\alpha_f = 0.98$) 80% ($\alpha_f = 0.8$) <80% ($\alpha_f \leqslant 0.8$) (linear increase)	2500 < F < 10,000 Hz 1000 < F < 2500 Hz 100 < F < 1000 Hz
Wall thickness	7.5 cm	

have internal dimensions 20 × 20 cm, 20 × 20 cm and 70 × 70 cm. The trapdoors are placed at middle panel height and their positions are indicated in Fig. 1a. A wooden access door of internal dimensions 70 × 200 cm (width × length) and thickness 4.5 cm, is installed to allow access inside the box for setting up the instrumentation. Acoustic foam is added to trapdoors and access door as well.

Besides insulation from outdoor noise sources, the presence of acoustic foam intends to avoid acoustic volume resonance frequencies which depend inversely upon the characteristic lengths of the resonating volume, indicated $L_{x,y,z}$ in Table 1.

Finally, note that, if required, the whole structure can be dismounted and remounted.

3. Performance and discussion

In the following, the flow and acoustic performances of the insulation box are evaluated for the aimed range of Reynolds and Mach numbers.

3.1. Flow performance

Confinement is known to influence the flow [13,6]. The influence of the reduced volume of the box on the flow is studied for a typical nozzle geometry of interest such as a free jet issuing from a round nozzle with diameter $d \leqslant 25$ mm [15]. The nozzle is placed central in a wall panel so that the degree of confinement is similar in all directions.

Jet development involves jet spreading. A spatial overview of the geometrical maximal jet spreading angle $\theta(x,y)$ is given as:

$$\theta\left(\frac{x}{y}\right) = \arctan\left(\frac{x}{y}\right), \tag{1}$$

with streamwise direction x and transverse direction y. The origin ($x = 0$, $y = 0$) is taken at the centre of the nozzle's exit. Based on a typical value of $d \leqslant 25$ mm and a far field expansion angle of $\theta = 9°$ it is seen that jet development can be studied in the near and far field up to $\geqslant 80d$ [13]. Consequently, the dimensions of the insulation box are satisfying with respect to jet development experiments.

Besides jet spreading, confinement is known to affect momentum conservation [13,6]. The momentum constraint M/M_0 is expressed as:

$$\frac{M}{M_0}\left(\frac{x}{d}\right) = \left[1 + \frac{16}{\pi K^2}\left(\frac{x}{d}\right)^2 \frac{A_0}{A_r}\right]^{-1}, \tag{2}$$

with tube exit diameter d, tube exit area $A_0 = \frac{1}{4}\pi d^2$, jet centreline distance downstream the tube exit x, A_r cross-sectional area of the room at a given x/d-location, total momentum M_0, local jet momentum M and centreline decay constant K. Thus to first order, the local momentum M in the jet-like part is diminished as x/d increases. Therefore, Eq. (2) can be used to estimate the return of momentum in the jet for given decay parameter and room size. A typical value of the decay parameter for a nozzle with exit diameter $d = 25$ mm yields $K = 5.9$ [15,5]. The two-dimensional cross-section of the box yields $A_r = 3.88$ m^2 using dimensions given in Table 1. The resulting momentum constraint M/M_0 is illustrated in Fig. 2. The streamwise distance is expressed with respect to the streamwise length L_x instead of to the nozzle diameter d, which facilitates interpretation regardless of the diameter d. It is easily seen that for the cross-section A_r a momentum loss in the jet smaller than 10%, 20% and 30% corresponds to streamwise positions of 45%, 65% and 85% of the streamwise length L_x. As a reference also values for half and twice the cross-sectional area A_r are shown, indicating that the streamwise extent is increased with 20% for $2 \times A_r$ and decreased with about 15% for $A_r/2$. Consequently, the current dimensions are judged to offer a good balance between cross-sectional area and momentum constraint since for $d \leqslant 25$ mm jet development can be studied up to $x/d \geqslant 36$ for $M/M_0 \geqslant 0.9$.

3.2. Acoustic performance

An omni directional microphone Bruel & Kjaer (type 4192) with associated pre-amplifier (B&K 4165) and additional amplifier ($0 \leqslant G \leqslant 50$ dB) and power supply (B&K 5935L) is used to perform sound measurements in the untreated room and in the insulation

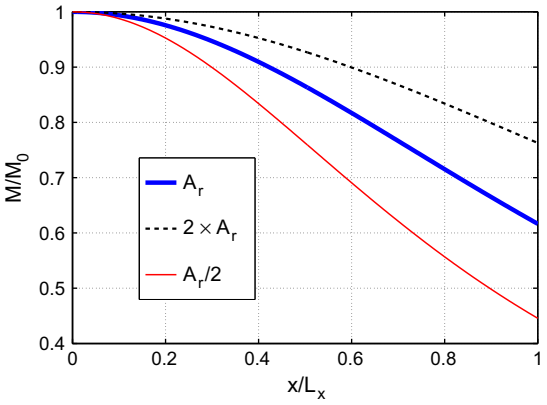

Fig. 2. Momentum constraint $M/M_0(x/L_x)$ for $d = 25$ mm, $K = 5.9$ and $A_r = 3.88$ m^2 (thick solid line), $2 \times A_r$ (dashed line), $A_r/2$ (thin solid line).

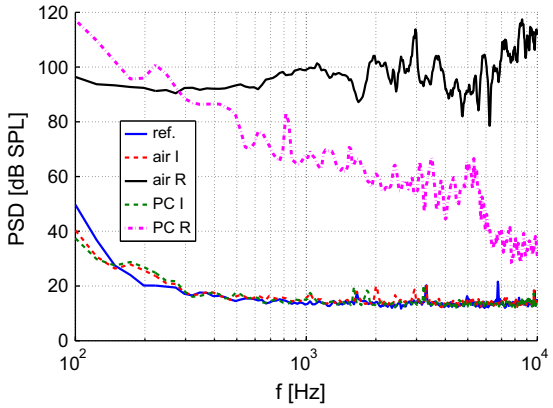

Fig. 3. Performance of the insulation box for typical background noises due to the measurement procedure: Power Spectral Density (PSD) for 110 l/min air supply and PC usage in the non-treated room (R) and in the insulation box (I).

box. Sounds are recorded during 10 s consecutively for steady sources at 2^{16} samples per second. The sensitivity of the microphone is determined with a calibrator (B&K 4231).

3.2.1. Attenuation of external sources

The acoustic performance is firstly evaluated with respect to unwanted noise sources which are inherent to the measurement procedure and to the flow facility. Signals are high-pass filtered with a fifth order Butterworth filter with cutoff frequency 100 Hz, so that the electrical network frequency of 50 Hz and low frequency noises are excluded. In addition, attenuation below 100 Hz is expected to be insufficient due to the poor attenuation of the foam as indicated in Table 1. All sound pressure levels are expressed in dB SPL as:

$$SPL = 20log_{10}\left(\frac{p_{rms}}{p_{ref}}\right), \tag{3}$$

where $p_{ref} = 2 \times 10^{-5}$ Pa and $p_{rms} = \sqrt{\frac{1}{N}\sum_{i=1}^{N} p_i^2}$, with p_i the ith instantaneous acoustic pressure out of $N = 655{,}360$ samples.

The attenuation of external noise sources is quantified using a simple additive model for the sound pressure level so that an unwanted source is considered to have no influence in case the difference between wanted and unwanted source ΔdB is more than 25 dB.

The attenuation of background noises measured inside and outside the insulation box due to airflow supply (180 l/min and 110 l/min) and PC usage is given in Table 2. In addition, the attenuation of human conversational speech is shown. SPL-values measured in the non-treated room are >80 dB for airflow supply, 68 dB for computer usage and 70 dB for the voice sample. Recall that the SPL level of the voice sample is within the range expected for human conversational speech [11]. The value of computer usage and voice are of the same order of magnitude whereas the SPL values measured for airflow supply are >10 dB larger, so that airflow supply is the most important source of background noise during the measurements. From Table 2 it is observed that corresponding attenuated values measured in the insulation box approximate the reference level of 36 dB. In addition, it is seen that all background noise sources are attenuated with more than 25 dB. Consequently, the attenuation of SPL for unwanted noise sources inherent to the measurement procedure and airflow supply is satisfactory.

Table 2
Performance of the insulation box for typical background noise due to the measurement procedure: measured sound pressure levels (SPL) for air supply (180 and 110 l/min) and PC usage in the non-treated room (R) and in the insulation box (I).

Noise	Measured SPL levels		
	Non-treated room (SPL_R)	Insulation box (SPL_I)	Attenuation ($SPL_R - SPL_I$)
180 l/min	92 dB	36 dB	>25 dB
110 l/min	82 dB	36 dB	>25 dB
PC	68 dB	37 dB	>25 dB
Voice	70 dB	38 dB	>25 dB
Reference level	36 dB		

Next, the spectral attenuation of the insulation box is considered. Fig. 3 illustrates the attenuation with respect to the reference level for unwanted noise sources inherent to the experimental procedure, *i.e.* airflow supply 110 l/min and PC usage. Both sources are broadband noises for which the spectrum covers the entire frequency domain when measured in the non-treated room. It is observed that the corresponding spectra measured inside the insulation box match the reference level for $f \geqslant 300$ Hz and that for $f < 300$ Hz the difference with the reference level is less than 10 dB. Note that despite the approximately square shape of the insulation box, the attenuation is independent of its acoustical modes. Consequently, as for the attenuation in SPL, the spectral attenuation of the insulation box for unwanted noise sources inherent to the measurement procedure and airflow supply is satisfying.

3.2.2. Acoustic behaviour

The homogeneity and reverberation time of the insulation box are estimated.

A driver unit of a horn speaker (SHOW/SKY TU-100) is used as a transducer for producing an arbitrary sound source. A cylindrical cone is mounted to the driver unit in order to generate a point source. Electrical signals are connected to a PC through a National Instruments BNC-2090 Card and a National Instruments (PCI-MIO-16XE-10) acquisition card. The sent/acquired data are processed using LabView 8 (National Instruments). Sinusoidal signals are fed to the driver unit. The frequencies of the sinusoidal signals are varied between 100 and 10 kHz with frequency steps of 25 Hz. The sound power of the source for all frequencies yields 53 ± 3 dB SWL when assuming a point source.

In order to evaluate the homogeneity of the insulation box different microphone positions are considered for a fixed source location in the centre of the box at a height of 18 cm above its floor. Measurement positions are symmetrical around the source

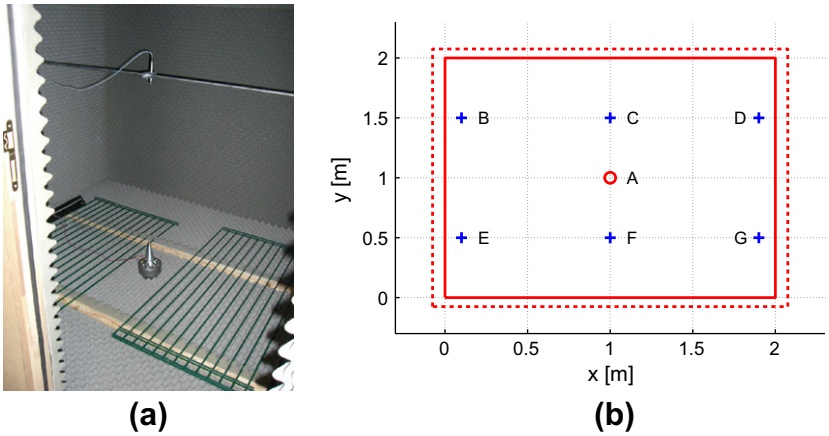

Fig. 4. (a) Overview of the installation of source and microphone. Grids are removed during the measurements. (b) Spatial overview of 6 microphone positions (+) in the plane corresponding to $L_z/2$ placed symmetrically around the central position of the point source (o labelled A) in the plane corresponding to 0.1 L_z. Positions B, D, E and G are at 1.32 m from the source and positions C and F are at 1.03 m from the source.

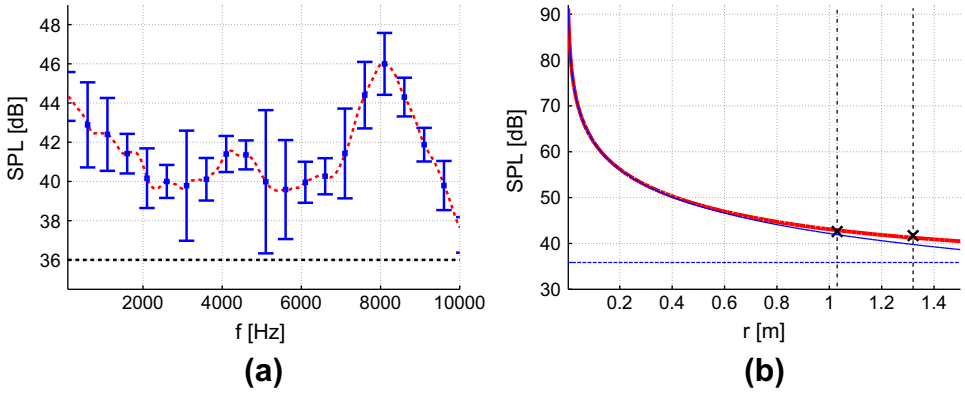

Fig. 5. (a) Mean and standard deviation as function of frequency for the measured SPL resulting from 4 different microphone positions at 1.32 m from the source as function of frequency f. The horizontal line indicates the background level. (b) Decay as function of distance d from source for a point source of 53 ± 3 dB SWL following (4) for $\alpha = 0.9$. The direct field (thin full line), diffuse field (horizontal line) and total field (thick full line) are indicated. Vertical dashed lines correspond to a distance of 1.03 and 1.32 m from the source. Values of the total dB SPL corresponding to the measurement positions are indicated (×).

position at half-height of the room at a distance of 1.32 and 1.03 m from the source as schematically indicated in Fig. 4.

The measured mean SPL levels as function of frequency for microphone positions at a distance of 1.32 m from the source are given in Fig. 5a and yield 41.7 ± 2.7 dB. The standard deviation for the different positions is indicated as well. The maximum standard deviation is less than 5 dB and its mean yields 1.7 dB corresponding to 4% of the mean dB value. For measurement positions at a distance of 1.03 m, the general tendency of the curve is maintained. The mean value for all frequencies increases to 43.0 ± 3.8 dB. In addition, the mean standard deviation for each frequency yields 1.5 dB corresponding to less than 4% of its mean value.

Consequently, the absorption coefficient varies depending on the frequency whereas spatial homogeneity for a given frequency has an accuracy of 4%. From the general tendency it is seen that absorption is reduced for frequencies less than 2500 Hz which is in accordance with the foam characteristics given in Table 1. In addition, absorption is observed to be reduced around 8100 Hz.

Fig. 5b illustrates the modelled decay of a point source as a function of distance r from the source [10,7]. As for experimental data, the source strength is set to 53 ± 3 dB SWL. The decay is modelled assuming uniform directivity as:

$$p^2_{rms}(W,S,\alpha,r) = \rho c\left(\frac{W}{4\pi r^2} + \frac{4W(1-\alpha)}{\alpha S}\right), \tag{4}$$

with total wall surface S, averaged absorption coefficient α, source power W and density of air ρ. The first term corresponds to the direct field the point source and the second term indicates the diffuse field. Recall that in (4) absorption due to air is neglected due to the small volume of the insulation box, so that for the highest frequency of 10 kHz the additional surface is less than 3% of S. Predicted dB SPL values for $0.8 \leqslant \alpha \leqslant 0.95$ provide an accurate estimation for measured mean dB SPL values as illustrated in Fig. 5b for $\alpha = 0.9$. Recall that $0.8 \leqslant \alpha \leqslant 0.95$ is in accordance with Table 1 for $f \geqslant 1000$ Hz. Corresponding reflection coefficients β are defined as $\beta^2 = 1 - \alpha$ so that $0.44 \geqslant \beta \geqslant 0.22$ holds.

The critical distance from the source $r_c(\alpha)$ for which the diffuse and direct field are of equal strength is estimated as:

$$r_c(S,\alpha) = \frac{\alpha S}{16\pi(1-\alpha)}. \tag{5}$$

The critical distance decreases rapidly with α, *e.g.* $r_c(\alpha = 0.9) = 4.1$ m, $r_c(\alpha = 0.8) = 1.8$ m and $r_c(\alpha = 0.7) = 1.1$ m, for a fixed value of S corresponding to the insulation box given in Table 1. Consequently, the sound field in the insulation box is not diffuse. Nevertheless, the reverberation time Tr, *i.e.* the time required for the sound pressure level to decrease by 60 dB [3,10], is estimated experimentally from the measured impulse response $h(t)$ of a balloon burst, illustrated in Fig. 6, by means of the Schroeder integral $E(t)$ as [10]:

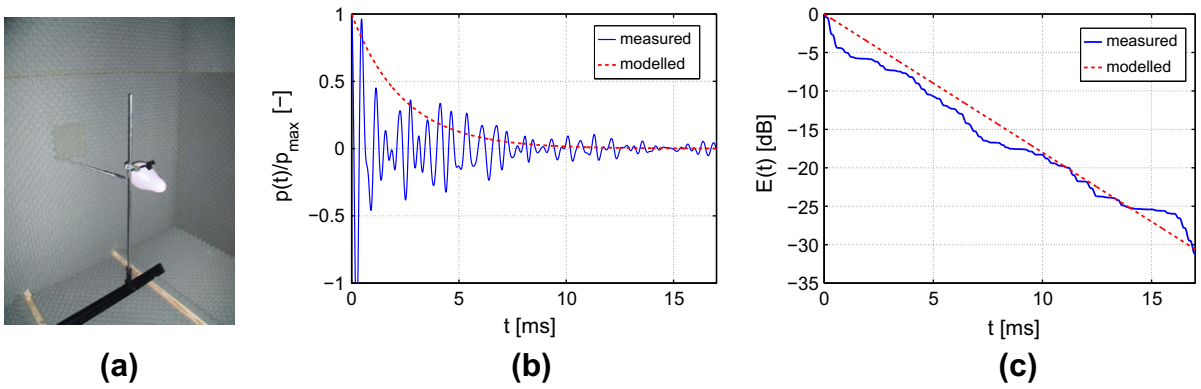

Fig. 6. (a) Illustration of setup used to generate an impulse response in the insulation box due to a balloon burst. A trapdoor is used to cause the balloon burst without an experimenter present. (b) Example of normalised measured impulse response $h(t)$ (full line) and modelled impulse response $\hat{h}(t) = e^{\frac{-13.8t}{Tr_m}}$ (dashed line). (c) Example of Schroeder integral $E(t)$ obtained from the measured (full line) and modelled (dashed line) impulse response.

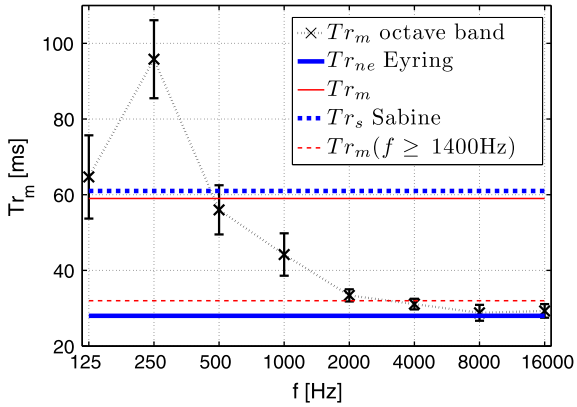

Fig. 7. Estimated mean (×) and standard deviation (vertical error bars) of the reverberation time Tr_m for each octave band in the range from 89 Hz up to 22.5 kHz. The centre frequency of each band is indicated. For comparison also the averaged measured Tr_m (thin full line), the averaged high-pass filtered $Tr_m(f \geqslant 1400\text{ Hz})$ (thin dashed line), modelled Tr_s (thick dashed line) and modelled Tr_{ne} (thick full line) are indicated.

$$E(t) = 10log_{10}\left(\int_t^{\infty} h^2(\tau)d\tau\right), \tag{6}$$

$$Tr_m = 60\text{ dB}\frac{t_{(-35\text{ dB})} - t_{(-5\text{ dB})}}{(-5\text{ dB}) - (-35\text{ dB})}, \tag{7}$$

where $t_{(-X\text{dB})}$ denotes the time when the energy decay $E(t)$ has decreased to XdB below its start value. The resulting reverberation time, estimated from 12 measured impulse responses, yields $Tr_m = 59 \pm 10$ ms. Denoting the measured mean value $\overline{Tr}_m = 59$ ms, the impulse is modelled as:

$$\hat{h}^2(t) = e^{\frac{-13.8t}{Tr_m}}, \tag{8}$$

since $10log_{10}(\hat{h}^2(t = Tr_m)) = -60$ dB.

In order to validate the influence of the absorption coefficients $\alpha(f)$, Fig. 7 illustrates the estimated Tr_m for each octave band in the range from 89 Hz up to 22.5 kHz. The low frequency range $f \leqslant 355$ Hz, corresponding to the first two octave bands, is characterised by large reverberation times $Tr > 60$ ms with high standard deviation of 17%. For octave bands with $f > 355$ Hz, the mean Tr_m and its standard deviation decreases gradually to reach $Tr_m(f \geqslant 1400\text{ Hz}) = 31 \pm 2$ ms and the standard deviation reduces to 6%. For intermediate frequencies $355 < f < 1400$ Hz, the reverberation time varies in the range $30 < Tr_m\,(355 < f < 1400\text{ Hz}) < 60$ ms. The retrieved values are summarised in Table 3. For comparison, estimations of the reverberation time by Sabine's equation $Tr_s(V, S, \alpha) = \frac{24Vlog(10)}{c\alpha S}$ [12], by Norris-Eyring theory $Tr_{ne} = -\frac{24Vlog(10)}{cSlog(1-\alpha)}$ [4] and by the image source method Tr_{ism} (ISM) [2,8] are summarised in Table 3 and indicated in Fig. 7. It is seen that Norris-Eyring estimation of the reverberation time is a good approximation for $f \geqslant 1400$ Hz and Sabine's formulation can be used for low frequencies $89 < f < 355$ Hz. Moreover, for $f \geqslant 1400$ Hz the reverberation time can be approximated by a constant value independent from frequency.

Finally, the Schroeder frequency F_c [3,14,9],

$$F_c = 2000\sqrt{\frac{Tr}{V}}, \tag{9}$$

based on the estimated reverberation time $30 \leqslant Tr \leqslant 60$ ms yields $125 \leqslant F_c \leqslant 180$ Hz. Consequently, statistical models can be used for $f \geqslant F_c$.

4. Conclusion

A non-expensive insulation box for aero-acoustic experiments at low Mach and moderate Reynolds numbers is integrated in an ordinary room equipped with air supply. Consequently, its design is a compromise between flow and acoustic experimental needs

Table 3
Overview of predicted and measured reverberation times Tr. Modelled values are obtained for an averaged absorption coefficient in the range $0.8 \leqslant \alpha \leqslant 0.95$.

	Symbol	Method	Value (ms)	Main error	Accuracy
Modelled	Tr_s	Sabine's equation	61 ± 5	Small V, high α	Overestimation
	Tr_{ne}	Norris-Eyring	28 ± 5	Overestimation α	Underestimation
	Tr_{ism}	Image source method	25 ± 5	Overestimation α	Underestimation
Measured	Tr_m	Impulse response	59 ± 10	Biased $E(t)$	Overestimation
		Filtered impulse response	31 ± 2	$f \geqslant 1400$ Hz	High f
Total	Tr		$30 \leqslant Tr \leqslant 60$		Order of magnitude

as well as practical limitations. The main characteristics of the insulation box can be summarised as follows:

- The insulation box has a volume of 7.45 m^3 and a total surface of 22.9 m^2. Absorbing foam is used in order to provide absorption in the frequency range from 100 Hz up to 10 kHz. If needed, the applied design allows the room to be displaced since it can be dismounted and remounted.
- The influence of the confinement due to the box on the flow is evaluated by considering jet development. It is seen that for the aimed range of Reynolds and Mach numbers the influence is negligible.
- The box insulates external broadband noises which are inherent to the aero-acoustic experimental setup and procedure such as noises due to the air supply regulation system and PC use.
- The homogeneity of measured dB SPL is estimated to have an accuracy of 4% for all frequencies in the interval 100 Hz up to 10 kHz. An averaged absorption coefficient is estimated from matching modelled and measured decay behaviour of a point source to be $0.8 \leqslant \alpha \leqslant 0.95$, which is in the characteristic range of the foam. The corresponding reflection coefficient varies in the range $0.44 \geqslant \beta \geqslant 0.22$. The critical distance for this range of absorption coefficients yields $r_c \geqslant 1.8$ m and the predicted reverberation time yields $Tr_{ne}(0.8 \leqslant \alpha \leqslant 0.95) \approx 28 \pm 5$ ms.
- From the measured and modelled Tr values, it is seen that the insulation box is characterised by a short reverberation time in the range $30 \leqslant Tr \leqslant 60$ ms, which can be approximated by a constant value $Tr \approx 31 \pm 2$ ms for frequencies $f \geqslant 1400$ Hz. The associated Schroeder frequency yields $125 \leqslant F_c \leqslant 180$ Hz.

Therefore, integration of the insulation box in an ordinary room equipped with air supply enables to perform aero-acoustic experiments at low Mach and moderate Reynolds numbers in acceptable flow and acoustic conditions.

References

[1] Elastomeres datasheet; 2010. <http://www.vente-technique.com>.
[2] Allen J, Berkley D. Image method for efficiently simulating small-rooms acoustics. J Acoust Soc Am 1979;65:943–50.
[3] Davis D, Davis C, editors. Sound system engineering. Sams & Co.; 1987.
[4] Eyring C. Reverberation time in 'dead' rooms. J Acoust Soc Am 1930;1:217–41.
[5] Grandchamp X. Modélisation physique des écoulements turbulents appliquée aux voies aériennes supérieures chez l'humain. PhD thesis, Grenoble Universities; 2009.
[6] Hussein H, Capp S, George W. Velocity measurements in a high Reynolds number momentum conserving axisymmetric turbulent jet. J Fluid Mech 1994;258:31–75.
[7] Kinsler LA, Frey AR, Coppens AB, Sanders JV. Fundamentals of acoustics. Wiley; 2000.
[8] Lehman E, Johansson A. Prediction of energy decay in room impulse responses simulated with an image-source model. J Acoust Soc Am 2008;124:269–77.
[9] Long M. Architectural acoustics. Elsevier; 2006.
[10] Rossing TD. Handbook of acoustics. Springer; 2007.
[11] Rossing TD, Moore FR, Wheeler PA, editors. The science of sound. Moore & Wheeler; 2002.
[12] Sabine W. Collected papers on acoustics. New York: Dover Publications; 1964.
[13] Schlichting H, Gersten K. Boundary layer theory. Berlin: Springer Verlag; 2000.
[14] Schroeder MR, Kutruff H. On frequency response curves in rooms. Comparison of experimental, theoretical, and Monte Carlo results for the average frequency spacing between maxima. J Acoust Soc Am 1962;34:76–80.
[15] Van Hirtum A, Grandchamp X, Pelorson X. Moderate Reynolds number axisymmetric jet development downstream an extended conical diffuser: influence of extension length. Eur J Mech – B/Fluids 2009;28:753–60.